Nonlinear Bending and Vibration Analysis of Imperfect Functionally Graded Microplate with Porosities Resting on Elastic Foundation Via the Modified Couple Stress Theory

Dang Van Hieu

Department of Mechanics, Thai Nguyen University of Technology, Thainguyen, Vietnam
E-mail: hieudv@tnut.edu.vn

Received 05 November 2021; Accepted 08 April 2022;
Publication 29 April 2022

Abstract

This paper represents the nonlinear bending and free vibration analysis of a simply supported imperfect functionally graded (FG) microplate resting on an elastic foundation based on the modified couple stress theory and the Kirchhoff plate theory (KPT) together with the von-Kármán's geometrical nonlinearity. The FG microplates with even and uneven distributions of porosities are considered. Analytical solutions for the nonlinear bending and free vibration are obtained. Comparing the obtained results with the published one in the literature shows the accuracy of the current solutions. Numerical examples are further presented to investigate the effects of the material length scale parameter to thickness ratio, the length to thickness ratio, the power-law index and the elastic foundation on the nonlinear bending and free vibration responses of the FG microplate.

Keywords: Microplate, functionally graded materials, nonlinear bending, modified couple stress theory, Kirchhoff plate theory.

European Journal of Computational Mechanics, Vol. 31_1, 101–126.
doi: 10.13052/ejcm2642-2085.3114

1 Introduction

Known as a kind of composite materials, FG materials with outstanding advantages compared to traditional composite materials are increasingly widely used in many industrial fields, especially in the aerospace industry, automotive industry, chemical industry, electronic industry and so on. Because of the wide applications of beam- and plate-like structures, the analysis of the mechanical responses of FG beams and plates has attracted the research interest of scientists [1, 2]. In recent years, the application of micro- and nano-sized structures has been increasing in the design of micro- and nano-sized devices and systems, especially in micro- and nano-electromechanical systems (MEMs/NEMs) [3, 4]. In MEMs/NEMs, besides fixed electrodes, movable parts are often modeled by micro-/nano-beams or micro-/nano-plates. Size-dependent effects have an important influence on the behaviors of micro-/nano-structures, so the classical elasticity theory is no longer suitable for modeling these small-sized structures because of the lack of material length scale parameters. Therefore, to observe the size-dependent effect on the mechanical behaviors of micro-/nano-structures, several non-classical elasticity theories have been proposed such as the nonlocal elasticity theory [5], the strain gradient theory [6], the couple stress theory [7–9] and the modified couple stress theory [10]. Among these size-dependent elasticity theories [5–10], the modified couple stress theory (MCST) has many advantages in computational practice because only one material length scale parameter is required.

Based on the MCST, some models of size-dependent micro-/nano-beams and plates were developed to observe the size-dependent effect on the mechanical behaviors of these small-sized structures. Ma et al. developed the models of size-dependent microbeams based on the Timoshenko beam theory [11], and the Reddy-Levinson beam theory [12] to investigate the static bending and free vibration problems. Şimşek [13] examined the nonlinear free vibration and static bending behaviors of the Euler-Bernoulli microbeam resting on the elastic foundation. The classical and first-order shear deformation theories were developed by Reddy and Berry [14] to study the nonlinear bending behavior of FG circular plates. The Ritz method was utilized by Ke et al. [15] to investigate the free linear vibration behaviors of size-dependent Mindlin microplates. Wang et al. [16] developed the Kirchhoff plate theory accounting for von-Kármán's geometrical nonlinearity to investigate the nonlinear free vibration behaviors of size-dependent circular microplates. The nonlinear free vibration behaviors of FG Mindlin microplates with the

von-Kármán's geometrical nonlinearity were represented by Ke et al. [17] and Ansari et al. [18]. The Reddy's plate theory was developed by Thai and Kim [19] to study the static bending and free linear vibration behaviors of FG plates. The analytical solutions for the problem of nonlinear static bending analysis of FG Kirchhoff and Mindlin plates were carried out by Thai and Choi [20] using Bubnov–Galerkin method. Lou and He [21] reported the analytical solutions for the nonlinear bending and free vibration analysis of FG microplates based on the Mindlin and Kirchhoff plate models. The static bending and forced vibration behaviors of an imperfect FG Mindlin microplate with porosities subjected to a moving load were investigated by Şimşek and Aydın [22] using Lagrange's method. Based on the MCST, the nonlinear vibration responses of FG microplates were investigated by Fan et al. [23] using the non-uniform rational B-spline-based isogeometric approach. The explicit solution for nonlinear free vibration of thin FG microplate based on the MCST and the KPT was reported by Setoodeh and Rezaei [24] using the Homotopy analysis method. And recently, Tao and Dai [25] presented the analysis of the size-dependent nonlinear free vibration of FG graphene platelets-reinforced composite annular sector microplates.

The problem of the static and dynamic analysis of size-dependent beams and plates based on the MCST has received much attention from researchers. However, the obtained results are mainly linear analyses. The results of the nonlinear analysis of the size-dependent plate models can be found in some works such as Wang et al. [16], Ke et al. [17], Ansari et al. [18], Thai and Choi [20], Lou and He [21], Fan et al. [23], Setoodeh and Rezaei [24] and Tao and Dai [25].

In this paper, author presents the analytical analysis of the nonlinear bending and free vibration behaviors of an imperfect FG microplate with porosities resting on an elastic foundation in the framework of the MCST and Kirchhoff plate model with the von-Kármán's geometrical nonlinearity. The simple power law is considered to estimate the material properties of the FG microplate. Along with that, two types of porosity distribution including even and uneven distributions are considered to examine the effect of porosities. The analytical solution for nonlinear bending and free vibration analysis of the imperfect FG microplate with porosities are carried out. The accuracy of the obtained solutions has been verified by comparison with the existing solutions. Numerical illustrations are given to evaluate the effects of several important parameters on the nonlinear deflection and frequency of the imperfect FG microplate.

2 Model and Formulation

A rectangular FG microplate with porosites resting on an elastic foundation is considered as shown in Figure 1. The FG microplate has the length *a*, width *b* and thickness *h*. The FG microplate is supported by an elastic foundation with linear and shear stiffness coefficients corresponding to k_L and k_P. The coordinate system (O*xyz*) is selected as in Figure 1.

The FG microplate composed of ceramic and metal is considered in this study. Where, the material properties of the FG microplate are assumed to vary continuously in the thickness direction. The upper surface of the FG microplate $(z = h/2)$ is assumed to be rich in ceramic, while the lower surface of the FG microplate $(z = -h/2)$ is assumed to be rich in metal. In addition, the effect of porosity is considered through two porosity distribution models including even distribution (FGM-I) and uneven distribution (FGM-II), as depicted in Figure 2. These models were proposed by Wattanasakulpong and Chaikittiratana [26] by modifying the rule of mixture.

For the even distribution of porosities inside the FG material which is defined as FGM-I, the material properties including the Young's modulus *E(z)* and the mass density $\rho(z)$ can be expressed as [26]:

$$E(z) = (E_c - E_m)\left(\frac{z}{h} + \frac{1}{2}\right)^k + E_m - (E_c + E_m)\frac{\delta}{2}, \tag{1}$$

$$\rho(z) = (\rho_c - \rho_m)\left(\frac{z}{h} + \frac{1}{2}\right)^k + \rho_m - (\rho_c + \rho_m)\frac{\delta}{2}. \tag{2}$$

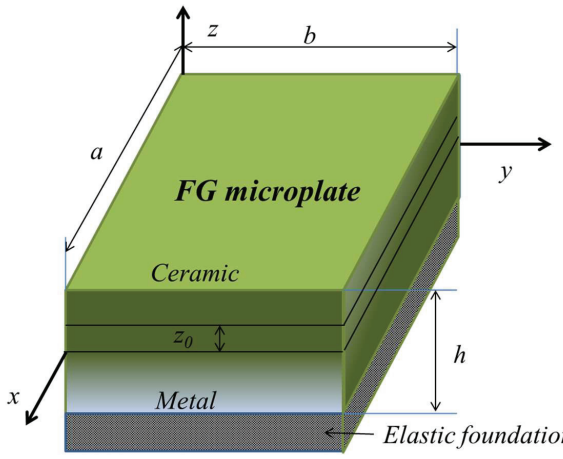

Figure 1 Model of an imperfect FG microplate resting on an elastic foundation.

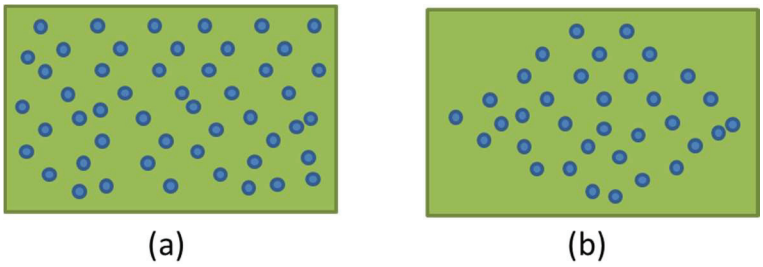

Figure 2 Two types of porosity distribution: (a) FGM-I and (b) FGM-II.

For the uneven distribution of porosities inside the FG material which is defined as FGM-II, the material properties can be expressed as [26]:

$$E(z) = (E_c - E_m)\left(\frac{z}{h} + \frac{1}{2}\right)^k + E_m - \frac{\delta}{2}(E_c + E_m)\left(1 - 2\frac{|z|}{h}\right), \quad (3)$$

$$\rho(z) = (\rho_c - \rho_m)\left(\frac{z}{h} + \frac{1}{2}\right)^k + \rho_m - \frac{\delta}{2}(\rho_c + \rho_m)\left(1 - 2\frac{|z|}{h}\right), \quad (4)$$

where, the non-negative number k ($0 \leq k < \infty$) is called the power-law index which governs the change in material properties of the FG microplate; and $\delta(0 < \delta \ll 1)$ indicates the porosity volume fraction. When $\delta = 0$ (without porosities), the imperfect FG microplate becomes to the perfect FG microplate. The FG microplate becomes a full ceramic microplate and full metal microplate corresponding to $k = 0$ and $k \to \infty$.

Because the effect of Poisson's ratio on the mechanical behaviors of FG structures is very small when compared with that of the Young's modulus and mass density [27]. Therefore, the Poisson's ratio ν is considered to be constant in this study.

For the imperfect FG microplate, the neutral surface and the mid-surface are not the same because of the elasticity modulus is anti-symmetric with respect to the mid-surface of the microplate. Therefore, it is necessary to consider the effect of the physical neutral surface. The position of the physical neutral surface can be determined as [21, 22]:

$$z_0 = \frac{\int_{-h/2}^{h/2} E(z) z \mathrm{d}z}{\int_{-h/2}^{h/2} E(z) \mathrm{d}z} \quad (5)$$

The displacement field of the FG microplate based on the Kirchhoff plate theory can be expressed as [21]:

$$\begin{cases} u_1(x,y,z,t) = u(x,y,t) - (z-z_0)\dfrac{\partial w}{\partial x} \\ u_2(x,y,z,t) = v(x,y,t) - (z-z_0)\dfrac{\partial w}{\partial y} \\ u_3(x,y,z,t) = w(x,y,t) \end{cases} \tag{6}$$

where (u, v, w) denote the displacements of a point on the physical neutral surface of the FG microplate. The non-zero components of the strain field of the FG microplate considering the von-Kármán's geometrical nonlinearity can be written as follows:

$$\begin{cases} \varepsilon_{xx} = \dfrac{\partial u}{\partial x} + \dfrac{1}{2}\left(\dfrac{\partial w}{\partial x}\right)^2 - (z-z_0)\dfrac{\partial^2 w}{\partial x^2} \\ \varepsilon_{yy} = \dfrac{\partial v}{\partial y} + \dfrac{1}{2}\left(\dfrac{\partial w}{\partial y}\right)^2 - (z-z_0)\dfrac{\partial^2 w}{\partial y^2} \\ \varepsilon_{xy} = \dfrac{\partial u}{\partial y} + \dfrac{\partial v}{\partial x} + \dfrac{\partial w}{\partial x}\dfrac{\partial w}{\partial y} - 2(z-z_0)\dfrac{\partial^2 w}{\partial x \partial y} \end{cases} \tag{7}$$

The components of the rotation vector can be expressed as [22]:

$$\theta_x = \frac{\partial w}{\partial y}, \quad \theta_y = -\frac{\partial w}{\partial x}, \quad \theta_{xy} = \frac{1}{2}\left(\frac{\partial v}{\partial x} - \frac{\partial u}{\partial y}\right), \tag{8}$$

The components of the symmetric curvature tensor are [20, 22]:

$$\begin{aligned} \chi_{xx} &= \frac{\partial^2 w}{\partial x \partial y}, \quad \chi_{yy} = -\frac{\partial^2 w}{\partial x \partial y}, \quad \chi_{zz} = 0, \\ \chi_{xy} &= \frac{1}{2}\left(\frac{\partial^2 w}{\partial y^2} - \frac{\partial^2 w}{\partial x^2}\right), \\ \chi_{xz} &= \frac{1}{4}\left(\frac{\partial^2 v}{\partial x^2} - \frac{\partial^2 u}{\partial x \partial y}\right), \\ \chi_{yz} &= \frac{1}{4}\left(\frac{\partial^2 v}{\partial x \partial y} - \frac{\partial^2 u}{\partial y^2}\right), \end{aligned} \tag{9}$$

The motion equations in terms of displacements (*u, v, w*) can be derived by employing the Hamilton's principle. The details for the process of establishing the motion equations of the FG microplate can be reviewed in the work of Thai and Choi [20]. Accordingly, with the elastic foundation, the equations of motion can be obtained as [21]:

$$A\left(\frac{\partial^2 u}{\partial x^2}+\frac{1-\nu}{2}\frac{\partial^2 u}{\partial y^2}+\frac{1+\nu}{2}\frac{\partial^2 v}{\partial x\partial y}\right)+\frac{A_n}{4}\nabla^2\left(\frac{\partial^2 v}{\partial x\partial y}-\frac{\partial^2 u}{\partial y^2}\right)$$
$$+A\left[\frac{\partial w}{\partial x}\frac{\partial^2 w}{\partial x^2}+\nu\frac{\partial w}{\partial y}\frac{\partial^2 w}{\partial x\partial y}+\frac{1-\nu}{2}\left(\frac{\partial w}{\partial y}\frac{\partial^2 w}{\partial x\partial y}+\frac{\partial w}{\partial x}\frac{\partial^2 w}{\partial y^2}\right)\right]$$
$$=I_0\frac{\partial^2 u}{\partial t^2}-I_1\frac{\partial^3 w}{\partial x\partial t^2}, \tag{10a}$$

$$A\left(\frac{\partial^2 v}{\partial y^2}+\frac{1-\nu}{2}\frac{\partial^2 v}{\partial x^2}+\frac{1+\nu}{2}\frac{\partial^2 u}{\partial x\partial y}\right)+\frac{A_n}{4}\nabla^2\left(\frac{\partial^2 u}{\partial x\partial y}-\frac{\partial^2 v}{\partial x^2}\right)$$
$$+A\left[\frac{\partial w}{\partial y}\frac{\partial^2 w}{\partial y^2}+\nu\frac{\partial w}{\partial x}\frac{\partial^2 w}{\partial x\partial y}+\frac{1-\nu}{2}\left(\frac{\partial w}{\partial x}\frac{\partial^2 w}{\partial x\partial y}+\frac{\partial w}{\partial y}\frac{\partial^2 w}{\partial x^2}\right)\right]$$
$$=I_0\frac{\partial^2 v}{\partial t^2}-I_1\frac{\partial^3 w}{\partial y\partial t^2}, \tag{10b}$$

$$-(D+A_n)\nabla^4 w+N(w)-k_L w+k_P\nabla^2 w-I_0\frac{\partial^2 w}{\partial t^2}$$
$$-I_1\left(\frac{\partial^3 u}{\partial x\partial t^2}+\frac{\partial^3 v}{\partial y\partial t^2}\right)+I_2\nabla^2\frac{\partial^2 w}{\partial t^2}=-q \tag{10c}$$

where, $q = q(x, y, t)$ is the distributed transverse force; (A, D) are the classical stretching coefficient and the bending stiffness coefficient, respectively; A_n is an additional stiffness due to the effect of the couple stress; and (I_0, I_1, I_2) denote the mass moments of inertia. These quantities are defined by:

$$(A, D)=\int_{-h/2}^{h/2}\frac{E(z)}{1-\nu^2}(1,(z-z_0)^2)dz,\quad A_n=l_m^2\frac{1-\nu}{2}A, \tag{11}$$

$$(I_0, I_1, I_2)=\int_{-h/2}^{h/2}\rho(z)(1,(z-z_0),(z-z_0)^2)dz, \tag{12}$$

where l_m is the material length scale parameter (MLSP) which reflects the effect of couple stress. In Equation (10c), the expression of $N(w)$ is:

$$N(w) = \frac{\partial}{\partial x}\left(N_x\frac{\partial w}{\partial x} + N_{xy}\frac{\partial w}{\partial y}\right) + \frac{\partial}{\partial y}\left(N_{xy}\frac{\partial w}{\partial x} + N_y\frac{\partial w}{\partial y}\right), \tag{13}$$

in which:

$$\begin{bmatrix} N_x \\ N_y \\ N_{xy} \end{bmatrix} = A \begin{bmatrix} 1 & \nu & 0 \\ \nu & 1 & 0 \\ 0 & 0 & \dfrac{1-\nu}{2} \end{bmatrix} \begin{bmatrix} \dfrac{\partial u}{\partial x} + \dfrac{1}{2}\left(\dfrac{\partial w}{\partial x}\right)^2 \\ \dfrac{\partial v}{\partial y} + \dfrac{1}{2}\left(\dfrac{\partial w}{\partial y}\right)^2 \\ \dfrac{\partial u}{\partial y} + \dfrac{\partial v}{\partial x} + \dfrac{\partial w}{\partial x}\dfrac{\partial w}{\partial y} \end{bmatrix} \tag{14}$$

It should be noted that when considering the effect of the physical neutral surface, the classical stretching-bending coupling stiffness equals to zero ($B = \int_{-h/2}^{h/2} \frac{E(z)(z-z_0)}{1-\nu^2} dz = 0$). Because the contribution of the first-order mass moment (I_1) is much smaller than that of the others (I_0 and I_2), therefore, in this work, the first-order mass moment is ignored.

Considering the FG microplate with all edges simply supported, the boundary conditions are described by:

$$\begin{aligned} &\text{at } x = 0 \quad \text{and} \quad a\text{: } u = w = 0, \quad \frac{\partial v}{\partial x} = 0, \quad \frac{\partial^2 w}{\partial x^2} = 0 \\ &\text{at } y = 0 \quad \text{and} \quad b\text{: } v = w = 0, \quad \frac{\partial u}{\partial y} = 0, \quad \frac{\partial^2 w}{\partial y^2} = 0 \end{aligned} \tag{15}$$

3 Analytical Solutions

For simply supported FG microplate, the solutions (*u, v, w*) are assumed to have the following form [28]:

$$\begin{cases} u(x,y,t) = \dfrac{1}{16}\displaystyle\sum_{m=1}^{\infty}\sum_{n=1}^{\infty} \alpha W_{mn}^2(t) \sin 2\alpha x \left(\cos 2\beta y - 1 + \nu\beta^2/\alpha^2\right) \\ v(x,y,t) = \dfrac{1}{16}\displaystyle\sum_{m=1}^{\infty}\sum_{n=1}^{\infty} \beta W_{mn}^2(t) \sin 2\beta y \left(\cos 2\alpha x - 1 + \nu\alpha^2/\beta^2\right) \\ w(x,y,t) = \displaystyle\sum_{m=1}^{\infty}\sum_{n=1}^{\infty} W_{mn}(t) \sin\alpha x \, \sin\beta y \end{cases} \tag{16}$$

where, $\alpha = m\pi/a$, and $\beta = n\pi/b$. It can be easily checked that the solutions (16) satisfy the boundary conditions of the FG microplate (15). The transverse load *q(x,y)* can be expanded in the double-Fourier sine series as:

$$q(x,y) = \sum_{m=1}^{\infty}\sum_{n=1}^{\infty} Q_{mn} \sin\alpha x \ \sin\beta y \tag{17}$$

where

$$Q_{mn} = \frac{4}{ab}\int_0^a \int_0^b q(x,y)\sin\alpha x \ \sin\beta y \, dx \, dy \tag{18}$$

For some typical loads, the coefficients Q_{mn} are given by [20, 21]:

$$Q_{mn} = \begin{cases} q_0 & \text{for sinusoidal load of intensity } q_0 \\ \dfrac{16q_0}{mn\pi^2} & \text{for uniform load of intensity } q_0 \\ \dfrac{4Q_0}{ab}\sin\dfrac{mx}{2}\sin\dfrac{ny}{2} & \text{for point load } Q_0 \text{ at the center} \end{cases} \tag{19}$$

Substituting Equations (16) and (17) into Equation (10), and applying the Bubnov–Galerkin approach, the following equation is obtained:

$$\begin{aligned} &[I_0 + I_2(\alpha^2+\beta^2)]\ddot{W}_{mn} \\ &\quad + [(D+A_n)\left(\alpha^2+\beta^2\right)^2 + k_L + k_P(\alpha^2+\beta^2)]W_{mn} \\ &\quad + \left\{\frac{A}{16}[4\nu\alpha^2\beta^2 + (3-\nu^2)(\alpha^4+\beta^4)]\right\} W_{mn}^3 = Q_{mn}. \end{aligned} \tag{20}$$

Equation (20) is a nonlinear ordinary differential equation, in the following sub-sections, this equation will be used to find the nonlinear deflection and frequency of the FG microplate.

3.1 Nonlinear Bending Solution

Firstly, the solution for nonlinear bending analysis will be found. For the static bending problem, $W_{mn} = \text{const}$, therefore, from Equation (20), the equation for the static bending analysis is reduced to:

$$\begin{aligned} &\left\{\frac{A}{16}[4\nu\alpha^2\beta^2 + (3-\nu^2)(\alpha^4+\beta^4)]\right\} W_{mn}^3 \\ &\quad + [(D+A_n)(\alpha^2+\beta^2)^2 + k_L + k_P(\alpha^2+\beta^2)]W_{mn} = Q_{mn}. \end{aligned} \tag{21}$$

Equation (21) is a quadratic equation, it has one real and two complex conjugate roots, in which the real root is the nonlinear deflection of the FG microplate:

$$W_{mn}^{NL} = -c\left(\frac{27}{2}\bar{Q}_{mn} + \frac{3}{2}\sqrt{12c^3 + 81\bar{Q}_{mn}^2}\right)^{-1/3} + \left(\frac{1}{2}\bar{Q}_{mn} + \frac{1}{18}\sqrt{12c^3 + 81\bar{Q}_{mn}^2}\right)^{1/3} \tag{22}$$

in which:

$$c = \frac{(D + A_n)(\alpha^2 + \beta^2)^2 + k_L + k_P(\alpha^2 + \beta^2)}{\frac{A}{16}\left[4\nu\alpha^2\beta^2 + (3 - \nu^2)(\alpha^4 + \beta^4)\right]}, \tag{23}$$

$$\bar{Q}_{mn} = \frac{Q_{mn}}{\frac{A}{16}\left[4\nu\alpha^2\beta^2 + (3 - \nu^2)(\alpha^4 + \beta^4)\right]}. \tag{24}$$

The linear deflection of the FG microplate can be derived from Equation (21):

$$W_{mn}^{L} = \frac{Q_{mn}}{(D + A_n)(\alpha^2 + \beta^2)^2 + k_L + k_P(\alpha^2 + \beta^2)}. \tag{25}$$

It can be observed that the effect of the von-Kármán's geometrical nonlinearity is expressed by the first term on the left-hand side of Equation (21). It should be emphasized that this shows the difference between nonlinear and linear deflections of the FG microplate. Also from Equations (22) and (25), it can be seen that the nonlinear and linear deflections of the FG microplate decrease as the linear stiffness (k_L) and the shear stiffness (k_P) of the elastic foundation increase.

3.2 Nonlinear Vibration Solution

Secondly, the solution for nonlinear vibration analysis will be determined in this sub-section. For the purpose of free vibration analysis, letting $Q_{mn} = 0$, Equation (20) leads to:

$$\left[I_0 + I_{-2}\left(\alpha^2 + \beta^2\right)\right]\ddot{W}_{mn} + \left[\left(D + A_n\right)\left(\alpha^2 + \beta^2\right)^2 + k_L + k_P\left(\alpha^2 + \beta^2\right)\right]W_{mn} + \left\{\frac{A}{16}\left[4\nu\alpha^2\beta^2 + (3 - \nu^2)(\alpha^4 + \beta^4)\right]\right\}W_{mn}^3 = 0. \tag{26}$$

Introducing the following new coefficients:

$$\begin{cases} \Gamma_1 = \dfrac{(D+A_n)(\alpha^2+\beta^2)^2 + k_L + k_P(\alpha^2+\beta^2)}{I_0 + I_2(\alpha^2+\beta^2)}, \\ \\ \Gamma_2 = \dfrac{\frac{A}{16}\left[4\nu\alpha^2\beta^2 + (3-\nu^2)(\alpha^4+\beta^4)\right]}{I_0 + I_2(\alpha^2+\beta^2)}. \end{cases} \tag{27}$$

By using Equation (27), the nonlinear ordinary differential Equation (26) is rewritten as:

$$\ddot{W}_{mn} + \Gamma_1 W_{mn} + \Gamma_2 W_{mn}^3 = 0. \tag{28}$$

It can be observed that Equation (28) is a cubic-Duffing nonlinear equation. The approximate solution of this equation can be found by many analytical methods [29]. In this work, the Hamiltonian Approach [30] is employed to find the approximate solution of this equation. Accordingly, the approximate nonlinear frequency of the FG microplate can be found as follows:

$$\omega_{NL} = \sqrt{\Gamma_1 + \frac{3}{4}\Gamma_2 W_{\max}^2} \tag{29}$$

where $W_{\max}$ is the amplitude of the FG microplate. Consider Equation (27), the expression of the nonlinear frequency can be obtained:

$$\omega_{NL} = \sqrt{\begin{array}{l} \dfrac{\left[(D+A_n)(\alpha^2+\beta^2)^2 + k_L + k_P(\alpha^2+\beta^2)\right]}{I_0 + I_2(\alpha^2+\beta^2)} \\ \\ \quad + \dfrac{3}{4}\dfrac{\left\{\frac{A}{16}\left[4\nu\alpha^2\beta^2 + (3-\nu^2)(\alpha^4+\beta^4)\right]\right\}}{I_0 + I_2(\alpha^2+\beta^2)} W_{\max}^2 \end{array}} \tag{30}$$

The linear frequency of the FG microplate can be derived from the expression of the nonlinear frequency (30) by letting $W_{\max} = 0$ as follows:

$$\omega_L = \sqrt{\frac{(D+A_n)(\alpha^2+\beta^2)^2 + k_L + k_P(\alpha^2+\beta^2)}{I_0 + I_2(\alpha^2+\beta^2)}}. \tag{31}$$

Clearly, the coefficients of the elastic foundation (k_L, and k_P) lead to an increase of the frequency of the FG microplate.

4 Numerical Results

4.1 Verification Study

Since the results for nonlinear bending and vibration of the imperfect FG microplate with porosities are not available in the literature, only the results for the perfect FG microplate are used to validate the obtained solutions. The obtained results are compared with those of Lou and He [21]. Note that the results for the perfect FG microplate can be recovered from the results for the imperfect FG microplate by letting the porosity volume fraction equal to zero ($\delta = 0$). In the verification study, the elastic foundation is not taken into account, and the material properties are chosen as below:

$$E_c = 14.4\ \text{GPa}, \quad E_m = 1.44\ \text{GPa}, \quad \rho_c = 12.2 \times 10^3\ \text{kg/m}^3,$$

$$\rho_m = 1.22 \times 10^3\ \text{kg/m}^3, \quad \nu = 0.38, \quad h = 17.6\ \mu\text{m}$$

Figure 3 shows the comparison of the dimensionless deflections (w/h) obtained in this work and those of Lou and He [21]. A very good agreement between the obtained results and those of Lou and He [21] can be

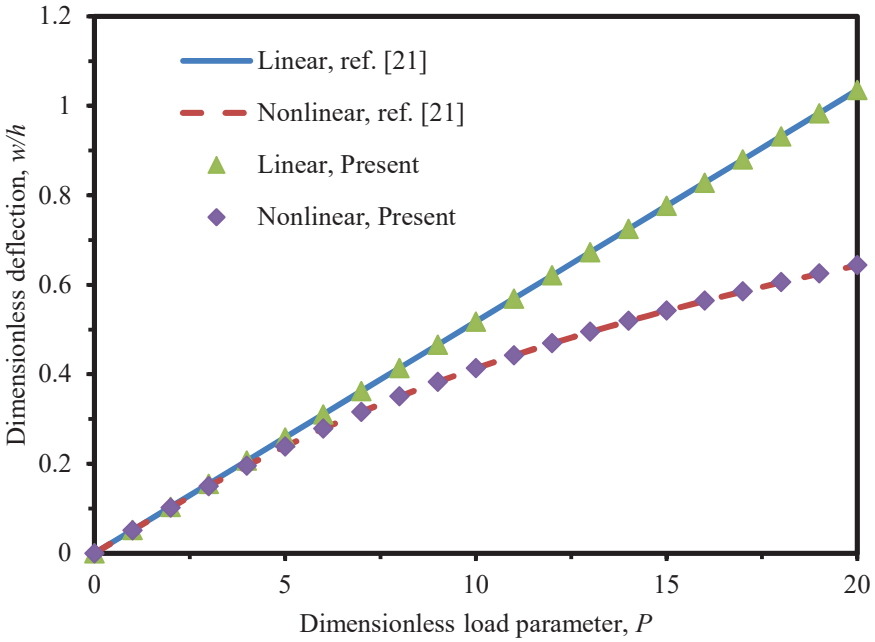

Figure 3 Comparison of dimensionless deflections of the perfect FG microplate ($a/h = 8$, $b = a$, $l_m/h = 0.2$, $k = 1$, and $q_0 = 1.0\ \text{N/m}^2$).

Table 1 Comparison of the dimensionless linear frequencies of the perfect FG microplate (a=10h, b=a)

	$k=0$		$k=2$		$k=5$	
l_m/h	Ref. [21]	Present	Ref. [21]	Present	Ref. [21]	Present
First mode ($m=1, n=1$)						
0	6.1103	6.1103	5.2254	5.2254	5.7296	5.7296
0.2	6.5491	6.5491	5.7346	5.7346	6.1964	6.1964
0.4	7.7174	7.7174	7.0445	7.0445	7.4226	7.4226
0.6	9.3453	9.3453	8.8049	8.8049	9.1065	9.1065
0.8	11.2349	11.2349	10.7975	10.7975	11.0405	11.0405
1.0	13.2749	13.2749	12.9154	12.9154	13.1146	13.1146
Second mode ($m=2, n=1$)						
0	15.0936	15.0936	12.9491	12.9491	14.1736	14.1736
0.2	16.1776	16.1776	14.2108	14.2108	15.3283	15.3283
0.4	19.0634	19.0634	17.4570	17.4570	18.3616	18.3616
0.6	23.0848	23.0848	21.8193	21.8193	22.5270	22.5270
0.8	27.7525	27.7525	26.7573	26.7573	27.3114	27.3114
1.0	32.7917	32.7917	32.0056	32.0056	32.4421	32.4421

observed from this figure. In this comparison, the dimensionless load parameter is defined as $P = \frac{q_0 a^4}{E_c h^4}$, where q_0 is the intensity of sinusoidal load. Table 1 shows the comparison of the dimensionless linear frequencies ($\bar{\omega} = \omega \frac{a^2}{h}\sqrt{\frac{\rho_m}{E_m}}$) for some values of the dimensionless MLSP (l_m/h). It can be seen that the obtained frequencies are the same as thoes of Lou and He [21].

The second comparative study was performed, the nonlinear frequencies of the FG microplate obtained in this work and those found by Fan et al. [23] using the non-uniform rational B-spline-based isogeometric technique are compared and the comparison is shown in Table 2. A good agreement between the present results and those obtained by Fan et al. [23] can be observed from Table 2. Note that the results obtained by Fan et al. [23] using the third-order shear deformation plate mode, so the results obtained in this work are slightly larger than the results of Fan et al. [23].

The third comparative study, the frequency ratios of the simply supported FG microplate obtained in this work and those of Setoodeh and Rezaei [24] using the Homotopy analysis method are compared and represented in Table 3 for some values of the dimensionless MLSP and dimensionless initial amplitude. The microplate composed of Al and Al_2O_3 is considered for this comparison. It can be observed that the results obtained in this work are very agreement with those achieved by Setoodeh and Rezaei [24].

Table 2 Comparison of dimensionless nonlinear frequencies of a simply supported square FG microplate

		$w_{\max}/h = 0.2$		$w_{\max}/h = 0.6$		$w_{\max}/h = 1.0$	
k	l_m/h	Present	Ref. [23]	Present	Ref. [23]	Present	Ref. [23]
1	0	5.5348	5.4121	6.5442	6.4416	8.1984	8.1181
	0.4	7.2757	7.1598	8.0703	7.9665	9.4613	9.3741
	0.8	10.9473	10.8237	11.4907	11.3733	12.5069	12.3998
5	0	5.8609	5.6707	6.8208	6.6594	8.4184	8.2906
	0.4	7.5244	7.3991	8.2940	8.1822	9.6507	9.5556
	0.8	11.1092	11.0201	11.6442	11.5595	12.6465	12.5691

Table 3 Comparison of dimensionless nonlinear frequencies of a simply supported square FG microplate ($a/h = 50, k = 2$)

	$w_{\max}/h = 0.2$		$w_{\max}/h = 0.6$		$w_{\max}/h = 1.0$	
h/l_m	Present	Ref. [24]	Present	Ref. [24]	Present	Ref. [24]
Classical	1.0229	1.0247	1.1903	1.2015	1.4689	1.4897
10	1.0218	1.0238	1.1820	1.1949	1.4503	1.4750
6	1.0202	1.0224	1.1690	1.1842	1.4207	1.4511
3	1.0149	1.0175	1.1267	1.1465	1.3222	1.3655
2	1.0103	1.0128	1.0894	1.1094	1.2324	1.2786
1	1.0039	1.0053	1.0346	1.0463	1.0933	1.1231

4.2 Parametric Study

In this sub-section, numerical illustrations are performed to evaluate the impact of some important parameters on the nonlinear bending and free vibration behaviors of the FG microplate with porosities. For this purpose, an FG microplate with the following material properties is considered:

$$E_c = 14.4\ \text{GPa}, \quad E_m = 1.44\ \text{GPa}, \quad \rho_c = 12.2 \times 10^3\ \text{kg/m}^3,$$

$$\rho_m = 1.22 \times 10^3\ \text{kg/m}^3, \quad \nu = 0.38, \quad h = 17.6\ \mu\text{m}$$

The dimensionless quantities are introduced:

$$\bar{w} = \frac{100E_m h^3}{q_0 a^4} w\left(\frac{a}{2}, \frac{b}{2}\right), \quad P = \frac{q_0 a^4}{E_c h^4}, \quad \Omega = \omega \frac{a^2}{h}\sqrt{\frac{\rho_m}{E_m}},$$

$$K_L = \frac{k_L a^4}{D}, \quad K_P = \frac{k_P a^2}{D}$$

Table 4 Dimensionless nonlinear deflection $\bar{w}_{\mathrm{NL}}$ of a square FG microplate (*Sinusoidal load*)

		$k=0$		$k=1$		$k=5$	
δ	l_m/h	FGM-I	FGM-II	FGM-I	FGM-II	FGM-I	FGM-II
0	0	0.2635	0.2635	0.6167	0.6167	1.2011	1.2011
	0.2	0.2294	0.2294	0.5176	0.5176	1.0270	1.0270
	0.4	0.1652	0.1652	0.3492	0.3492	0.7157	0.7157
	0.6	0.1126	0.1126	0.2264	0.2264	0.4755	0.4755
	0.8	0.0779	0.0779	0.1517	0.1517	0.3235	0.3235
	1	0.0558	0.0558	0.1065	0.1065	0.2293	0.2293
0.02	0	0.2664	0.2642	0.6368	0.6225	1.3042	1.2340
	0.2	0.2319	0.2301	0.5334	0.5225	1.1090	1.0544
	0.4	0.1670	0.1658	0.3587	0.3526	0.7653	0.7339
	0.6	0.1139	0.1131	0.2320	0.2286	0.5047	0.4871
	0.8	0.0788	0.0783	0.1553	0.1532	0.3417	0.3312
	1	0.0564	0.0561	0.1089	0.1076	0.2415	0.2346
0.04	0	0.2694	0.2650	0.6585	0.6285	1.4314	1.2696
	0.2	0.2345	0.2308	0.5504	0.5276	1.2086	1.0839
	0.4	0.1689	0.1664	0.3688	0.3561	0.8240	0.7533
	0.6	0.1152	0.1136	0.2380	0.2309	0.5384	0.4994
	0.8	0.0797	0.0787	0.1590	0.1548	0.3625	0.3393
	1	0.0571	0.0564	0.1115	0.1087	0.2553	0.2403

4.2.1 Bending

Tables 4 and 5 show the effects of the power-law index k, the porosity volume fraction δ and the dimensionless MLSP l_m/h on the dimensionless nonlinear deflection of the square FG microplate with sinusoidal and uniform loads, respectively. Input data is selected as $a = 20h$ and $q_0 = 1$ N/m^2; and the elastic foundation is not considered. It can be observed that when $\delta = 0$ (without the porosities), the imperfect FG microplate becomes to the perfect FG microplate; therefore, the results for the FGM-I microplate are equal to those for the FGM-II microplate. With the porosities ($\delta \neq 0$), the dimensionless nonlinear deflection of the imperfect FG microplate increases as the power-law index k and the porosity volume fraction δ increase, and reduces if increasing the dimensionless MLSP l_m/h. As expected, when the porosities are considered, the dimensionless deflection of the imperfect FG microplate is always larger than that of the perfect FG microplate. Tables 4 and 5 reveal that the dimensionless nonlinear deflections of the FGM-II microplate are always smaller than those of the FGM-I microplate. It means

Table 5 Dimensionless nonlinear deflection $\bar{w}_{\mathrm{NL}}$ of a square FG microplate (*Uniform load*)

		$k=0$		$k=1$		$k=5$	
δ	l_m/h	FGM-I	FGM-II	FGM-I	FGM-II	FGM-I	FGM-II
0	0	0.4272	0.4272	0.9998	0.9998	1.9472	1.9472
	0.2	0.3719	0.3719	0.8391	0.8391	1.6649	1.6649
	0.4	0.2678	0.2678	0.5661	0.5661	1.1602	1.1602
	0.6	0.1826	0.1826	0.3670	0.3670	0.7708	0.7708
	0.8	0.1264	0.1264	0.2460	0.2460	0.5244	0.5244
	1	0.0905	0.0905	0.1727	0.1727	0.3717	0.3717
0.02	0	0.4319	0.4284	1.0324	1.0092	2.1143	2.0005
	0.2	0.3760	0.3730	0.8648	0.8471	1.7978	1.7093
	0.4	0.2708	0.2688	0.5815	0.5716	1.2407	1.1897
	0.6	0.1846	0.1834	0.3762	0.3707	0.8182	0.7897
	0.8	0.1278	0.1270	0.2517	0.2484	0.5540	0.5369
	1	0.0915	0.0910	0.1766	0.1744	0.3915	0.3804
0.04	0	0.4368	0.4295	1.0675	1.0189	2.3204	2.0582
	0.2	0.3802	0.3742	0.8923	0.8553	1.9594	1.7571
	0.4	0.2783	0.2689	0.5979	0.5772	1.3258	1.2212
	0.6	0.1867	0.1842	0.3858	0.3744	0.8728	0.8096
	0.8	0.1292	0.1276	0.2578	0.2509	0.5877	0.5501
	1	0.0925	0.0914	0.1807	0.1762	0.4138	0.3895

that with porosity phases spreading mostly around the middle zone of the cross-section and the amount of porosities decrease linearly to zero at the top and bottom of the cross-section, the FGM-II microplate has a greater stiffness than the FGM-I microplate; therefore, the deflections of the FGM-II microplate are less than those of the FGM-I microplate. These results is useful for estimating the reliability of size-dependent FG microplate models developed in the future.

To illustrate the effect of the geometrical nonlinearity on the static bending response of the imperfect FG microplate, Figure 4 represents the load–deflection curves for an imperfect FG microplate. This figure is plotted with $a = 15h, b = a, l_m/h = 0.2, \delta = 0.1$, and the elastic foundation is not considered. Two cases including the sinusoidal and uniform loads are examined to plot this figure. This figure reveals that the nonlinear deflection is smaller than the linear one with the same applied load. This phenomenon can be explained by the intrinsic stiffening effect when considering the effect of geometrical nonlinearity. The difference between the linear and nonlinear deflections becomes more obvious as increasing value of applied load.

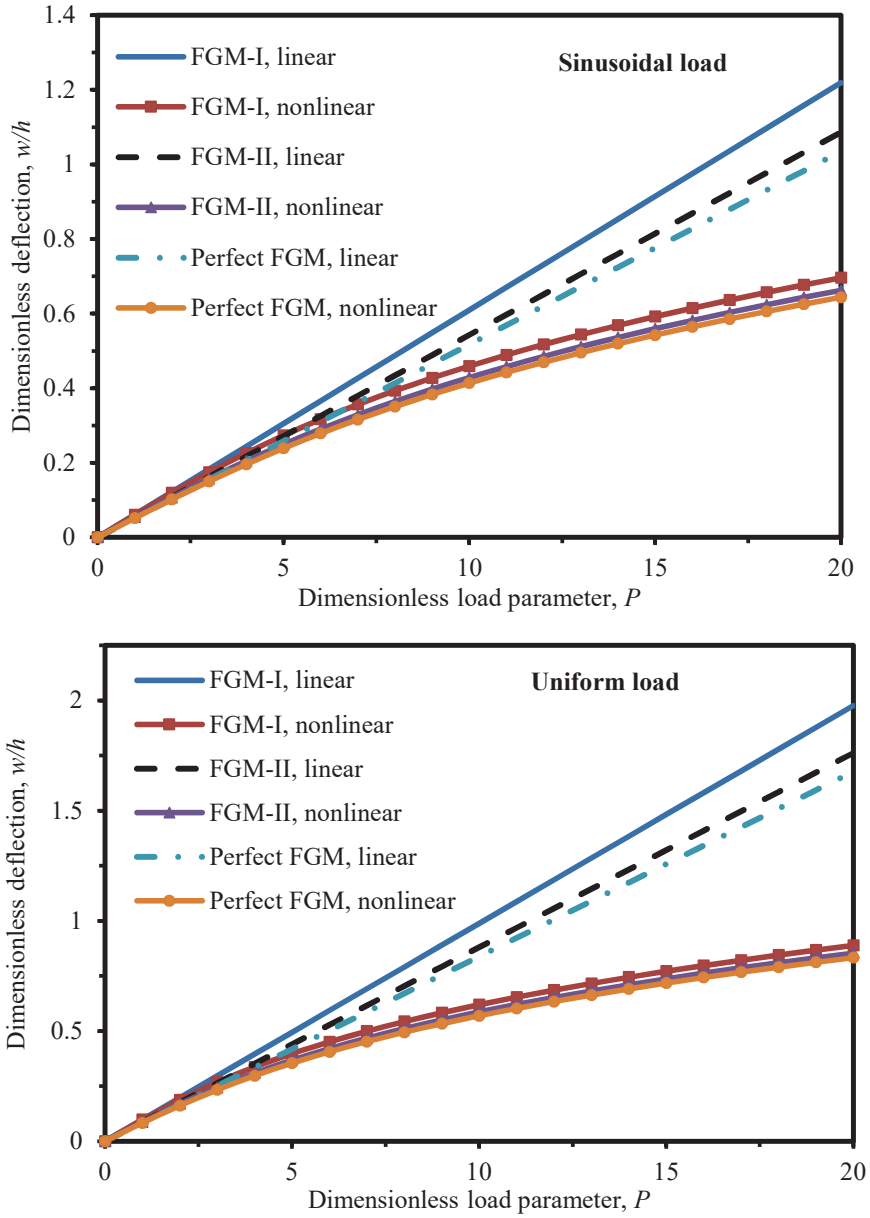

Figure 4 Linear and nonlinear deflections of the imperfect FG microplate.

Table 6 Dimensionless nonlinear deflection $\bar{w}_{\mathrm{NL}}$ of a square FG microplate (*Sinusoidal load*)

		$K_L = 0,\ K_P = 0$		$K_L = 10,\ K_P = 0$		$K_L = 10,\ K_P = 10$	
k	δ	FGM-I	FGM-II	FGM-I	FGM-II	FGM-I	FGM-II
0	0	0.2541	0.2541	0.2479	0.2479	0.1679	0.1679
	0.02	0.2569	0.2548	0.2507	0.2486	0.1698	0.1684
	0.05	0.2612	0.2559	0.2549	0.2497	0.1726	0.1691
	0.1	0.2688	0.2577	0.2624	0.2515	0.1777	0.1703
1	0	0.5885	0.5885	0.5745	0.5745	0.3903	0.3940
	0.02	0.6074	0.5941	0.5929	0.5799	0.4029	0.3997
	0.05	0.6384	0.6027	0.6232	0.5883	0.4236	0.4097
	0.1	0.6989	0.6178	0.6822	0.6031	0.4640	0.7628
5	0	1.1523	1.1523	1.1246	1.1246	0.7628	0.7836
	0.02	1.2492	1.1836	1.2192	1.1552	0.8279	0.8180
	0.05	1.4388	1.2355	1.4044	1.2058	0.9540	0.8864
	0.1	1.9844	1.3384	1.9374	1.3062	1.3201	

Table 7 Dimensionless nonlinear deflection $\bar{w}_{\mathrm{NL}}$of a square FG microplate (*Uniform load*)

		$K_L = 0,\ K_P = 0$		$K_L = 10,\ K_P = 0$		$K_L = 10,\ K_P = 10$	
k	δ	FGM-I	FGM-II	FGM-I	FGM-II	FGM-I	FGM-II
0	0	0.4119	0.4119	0.4019	0.4019	0.2722	0.2722
	0.02	0.4164	0.4130	0.4064	0.4031	0.2752	0.2730
	0.05	0.4235	0.4148	0.4133	0.4048	0.2799	0.2741
	0.1	0.4358	0.4178	0.4253	0.4077	0.2880	0.2761
1	0	0.9541	0.9541	0.9313	0.9313	0.6327	0.6327
	0.02	0.9847	0.9631	0.9612	0.9401	0.6531	0.6387
	0.05	1.0350	0.9771	1.0103	0.9537	0.6867	0.6479
	0.1	1.1330	1.0016	1.1060	0.9776	0.7522	0.6642
5	0	1.8680	1.8680	1.8231	1.8231	1.2366	1.2366
	0.02	2.0252	1.9188	1.9766	1.8727	1.3413	1.2703
	0.05	2.3326	2.0029	2.2768	1.9548	1.5466	1.3261
	0.1	3.2170	2.1697	3.1408	2.1176	2.1401	1.4370

The effect of the elastic foundation on the nonlinear deflection of the imperfect FG microplate is represented in Tables 6 and 7 for sinusoidal load and uniform load, respectively. These Tables are carried out with $a = 10h$, and $l_m/h = 0.1$. It is clearly that the stiffness coefficients lead to an increase of the nonlinear deflection of the imperfect FG microplate.

4.2.2 Vibration

The effect of the porosity volume fraction δ on the vibration behavior of the FG microplate is presented in Figure 5. This figure is plotted with $k = 5$, $l_m/h = 0.2$, $a = 8h$, $b = a$ and $K_L = K_P = 0$. It can be observed that the linear frequencies of the FG microplate are independent of the initial amplitude, while nonlinear frequencies of the FG microplate increase as the initial amplitude increases. This figure also reveals that the frequencies of the imperfect FG microplate are always larger than those of the perfect FG microplate. In contrast to the results for the static bending problem, the frequencies of the FGM-II microplate are always larger than those of the FGM-I microplate.

Figure 6 shows the effect of the power-law index k on the nonlinear vibration behavior of the imperfect FG microplate. This figure is plotted with the input data as $a = 8h$, $b = a$, $l_m = 0.2h$, $w_{\max}/h = 0.2$ and without the elastic foundation. It can be observed that the power-law index k has a rather

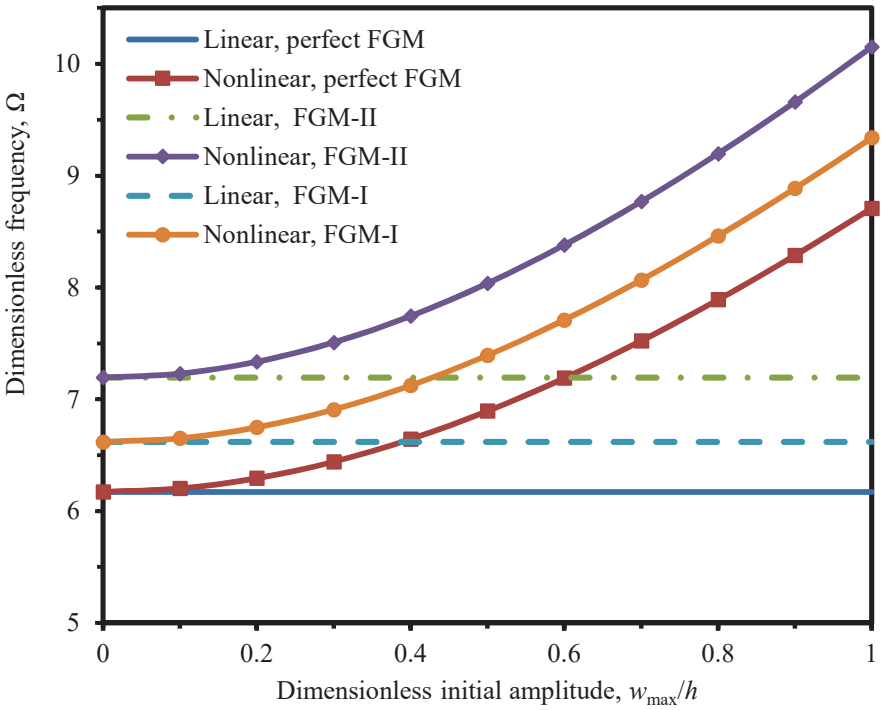

Figure 5 Variation of the dimensionless frequency to the dimensionless initial amplitude.

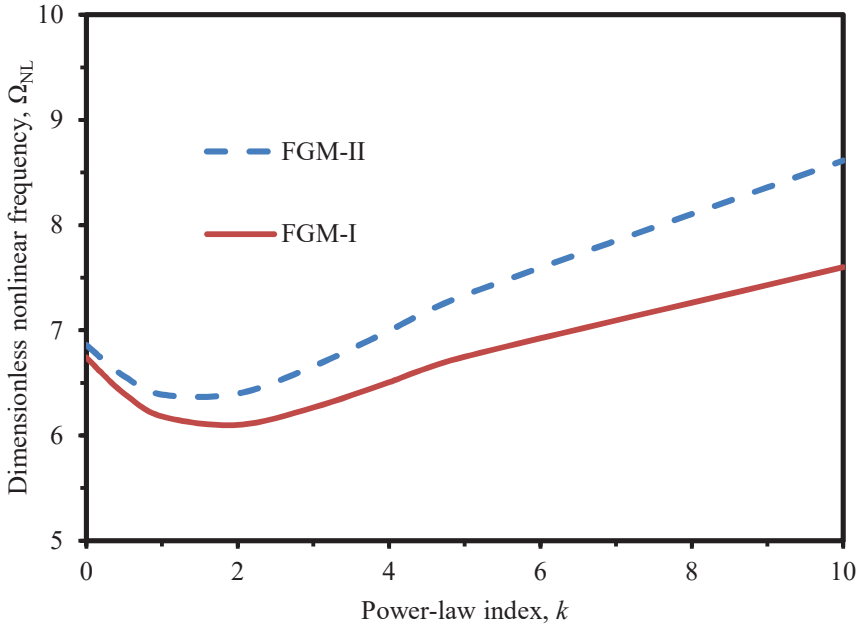

Figure 6 The effect of the power-law index k on the nonlinear vibration of the imperfect FG microplate.

interesting effect on the vibration response of the imperfect FG microplate. The nonlinear frequencies of the imperfect FG microplate initially decrease to their minimum values with increasing the power-law index, then increase again as value of the power-law index continues to increase.

With case of $a = 20h$, $b = a$, $k = 5$, $w_{\max}/h = 0.1$ and $K_L = K_P = 0$, Figure 7 shows the effect of the dimensionless MLSP l_m/h on the nonlinear vibration behavior of the imperfect FG microplate. It can be concluded that MLSP has a great influence on the vibration response of the imperfect FG microplate. In the framework of the modified couple stress theory [10], the MLSP enhances the stiffness of the imperfect FG microplate; therefore, the dimensionless nonlinear frequency of the imperfect FG microplate increases when the dimensionless MLSP increases.

Final, the effect of the elastic foundation on the nonlinear vibration behavior of the imperfect FG microplate is also examined and presented in Figures 8 and 9. With case of $a = 20h$, $b = a$, $l_m = 0.1h$, $k = 5$, $w_{\max}/h = 0.1$, and $K_P = 0$, the effect of the dimensionless linear stiffness coefficient K_L on the dimensionless frequency of the imperfect FG microplate is shown

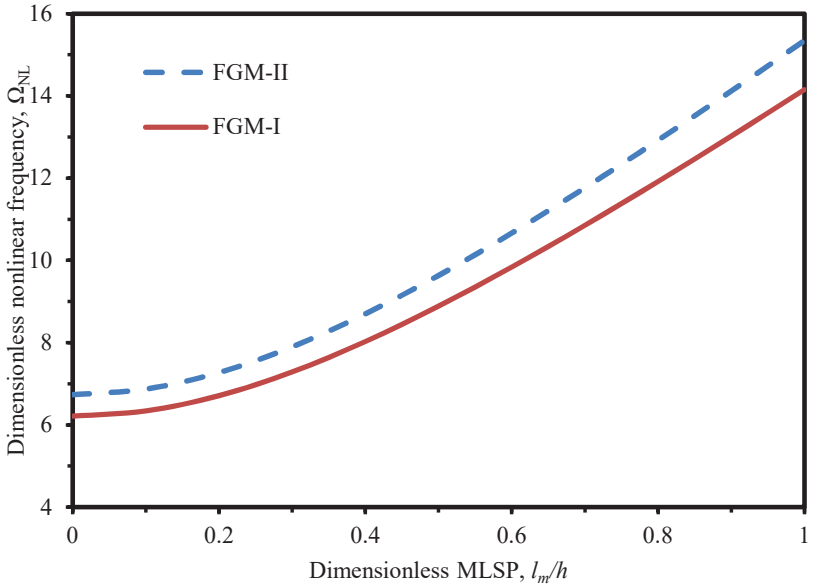

Figure 7 The effect of the dimensionless MLSP l_m/h on the nonlinear vibration of the imperfect FG microplate.

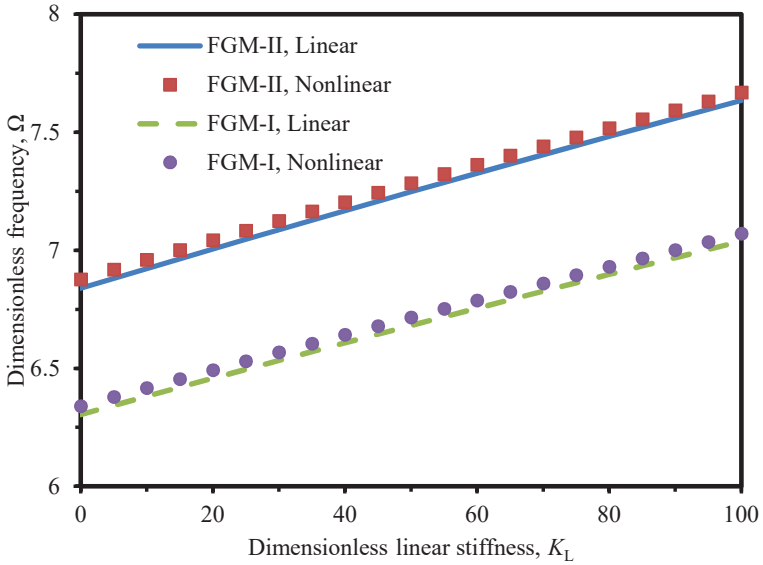

Figure 8 The effect of linear stifness coefficient on the vibration of the imperfect FG microplate.

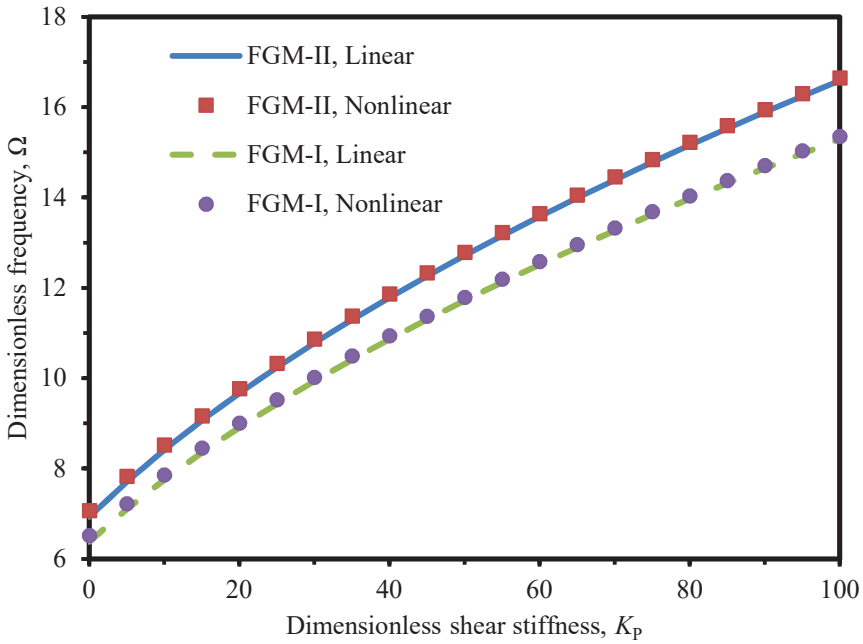

Figure 9 The effect of shear stifness coefficient on the vibration of the imperfect FG microplate.

in Figure 8. And Figure 9 shows the effect of the dimensionless shear stiffness coefficient K_P on the dimensionless frequency of the imperfect FG microplate with $a = 20h$, $b = a$, $l_m = 0.1h$, $k = 5$, $w_{\max}/h = 0.2$, and $K_L = 10$. As expected, the frequency of the imperfect FG microplate increases with increasing value of the elastic foundation parameters because the elastic foundation increases the stiffness of the imperfect FG microplate.

5 Conclusions

A size-dependent plate model based on the KPT with the von-Kármán's geometrical nonlinearity and the MCST was developed to examine the nonlinear bending and free vibration behaviors of S-S imperfect FG microplates with porosities resting on an elastic foundation. The solutions for the nonlinear deflection and free frequency of the imperfect FG microplate are obtained in the analytical forms. The numerical results are performed to evaluate the reliability of the obtained solutions as well as study the influence of important

parameters on the nonlinear free vibration and bending behaviors of the imperfect FG microplate. Some important conclusions can be summarized as follows:

- Because the geometrical nonlinearity of the microplate is considered, the nonlinear deflection of the microplate is less than the linear one at the same load, while the nonlinear frequency is larger than the linear one for the same initial amplitude.
- Both the nonlinear deflection and frequency of the imperfect FG microplate are always larger than those of the perfect FG microplate. The nonlinear deflection increases by increasing the power-law index and porosity volume fraction. The power-law index has an interesting effect on the vibration response of the microplate.
- The couple stress effect is more significant for the microplate with a larger value of the ratio l_m/h. The MLSP enhances the stiffness of the microplate; thereore, when the MLSP increases, the nonlinear deflection reduces and the nonlinear frequency increases.
- The nonlinear frequency increases with increasing value of the elastic foundation parameters; while the nonlinear deflection reduces by increasing value of the elastic foundation parameters.

Acknowledgements

This work is supported by Thai Nguyen University of Technology (TNUT).

References

[1] P. Zahedinejad, C. Zhang, H. Zhang and S. Ju. 'A Comprehensive Review on Vibration Analysis of Functionally Graded Beams', International Journal of Structural Stability and Dynamics, 20(4), 2030002, 2020.

[2] D.K. Jha, T. Kant, R.K. Singh, 'A critical review of recent research on functionally graded plates', Composite Structures, 96, pp. 833–849, 2013.

[3] A.S. Algamili, M.H.M.Khir, J.O. Dennis, et al. 'A Review of Actuation and Sensing Mechanisms in MEMS-Based Sensor Devices', Nanoscale Research Letters, 16, 16, 2021. https://doi.org/10.1186/s11671-021-03481-7

[4] W.M. Zhang, H. Yan, Z.K. Peng, G. Meng, 'Electrostatic pull-in instability in MEMS/NEMS: A review', Sensors and Actuators A, 214, pp. 187–218, 2014.
[5] A.C. 'Eringen Nonlocal polar elastic continua', International Journal of Engineering Science, 10(1), pp. 1–16, 1972.
[6] D.C.C. Lam, F. Yang, A.C.M. Chong, J. Wang J, P. Tong, 'Experiments and theory in strain gradient elasticity', Journal of the Mechanics and Physics of Solids, 51(8), pp. 1477–1508, 2003.
[7] R.D. Mindlin, H.F. Tiersten, 'Effects of couple-stresses in linear elasticity', Archive for Rational Mechanics and Analysis, 11(1), pp. 415–448, 1962.
[8] R.A. Toupin, 'Elastic materials with couple-stresses'. Archive for Rational Mechanics and Analysis, 11(1), pp. 385–414, 1962.
[9] W.T. Koiter, 'Couple stresses in the theory of elasticity, I and II', Philosophical Transactions of the Royal Society of London B, 67, pp. 17–44, 1964.
[10] F. Yang, A.C.M. Chong, D.C.C. Lam, P. Tong, 'Couple stress based strain gradient theory for elasticity', International Journal of Solids and Structures, 39(10), pp. 2731–2743, 2002.
[11] H.M. Ma, X.L. Gao, J.N. Reddy, 'A microstructure-dependent Timoshenko beam model based on a modified couple stress theory', Journal of the Mechanics and Physics of Solids, 56, pp. 3379–3391, 2008.
[12] H.M. Ma, X.L. Gao, J.N. Reddy, 'A nonclassical Reddy–Levinson beam model based on a modified couple stress theory', International Journal for Multiscale Computational Engineering, 8, pp. 167–180, 2010.
[13] M. Şimşek, 'Nonlinear static and free vibration analysis of microbeams based on the nonlinear elastic foundation using modified couple stress theory and He's variational method', Composite Structures, 112, pp. 264–272, 2014.
[14] J.N. Reddy, J. Berry, 'Nonlinear theories of axisymmetric bending of functionally graded circular plates with modified couple stress', Composite Structures, 94(12), pp. 3664–3668, 2012.
[15] L.L. Ke, Y.S. Wang, J. Yang, S. Kitipornchai, 'Free vibration of size-dependent Mindlin microplates based on the modified couple stress theory', Journal of Sound and Vibration, 331, pp. 94–106, 2012.
[16] Y.G. Wang, W.H. Lin, N. Liu, 'Large amplitude free vibration of size-dependent circular microplates based on the modified couple stress theory'. International Journal of Mechanical Sciences, 71, pp. 51–57, 2013.

[17] L.L. Ke, J. Yang, S. Kitipornchai, M.A. Bradford, Y.S. Wang, 'Axisymmetric nonlinear free vibration of size-dependent functionally graded annular microplates', Composites Part B: Engineering, 53, pp. 207–217, 2013.

[18] R. Ansari, M.F. Shojaei, V. Mohammadi, R. Gholami, M.A. Darabi, 'Nonlinear vibrations of functionally graded Mindlin microplates based on the modified couple stress theory'. Composite Structures, 114, pp. 124–134, 2014.

[19] H.T. Thai, S.E. Kim, 'A size-dependent functionally graded Reddy plate model based on a modified couple stress theory', Composites Part B: Engineering, 45, pp. 1636–1645, 2013.

[20] H.T. Thai, D.H. Choi, 'Size-dependent functionally graded Kirchhoff and Mindlin plate models based on a modified couple stress theory', Composite Structures, 95, pp. 142–153, 2013.

[21] J. Lou, L. He, 'Closed-form solutions for nonlinear bending and free vibration of functionally graded microplates based on the modified couple stress theory', Composite Structures, 131, pp. 810–8201, 2015.

[22] M. Şimşek, M. Aydın, 'Size-Dependent Forced Vibration of an Imperfect Functionally Graded (FG) Microplate with Porosities Subjected to a Moving Load Using the Modified Couple Stress Theory', Composite Structures, 160, pp. 408-421, 2017.

[23] F. Fan, Y. Xu, S. Sahmani, B. Safaei, 'Modified couple stress-based geometrically nonlinear oscillations of porous functionally graded microplates using NURBS-based isogeometric approach', Computer Methods in Applied Mechanics and Engineering, 372, 113400, 2020.

[24] A.R. Setoodeh and M. Rezaei, 'An explicit solution for the size-dependent large amplitude transverse vibration of thin functionally graded micro-plates', Scientia Iranica B, 25(2), 799–812, 2018.

[25] C. Tao, T. Dai, 'Isogeometric analysis for size-dependent nonlinear free vibration of graphene platelet reinforced laminated annular sector microplates', European Journal of Mechanics/A Solids, 86, 104171, 2021.

[26] N. Wattanasakulpong, A. Chaikittiratana, 'Flexural vibration of imperfect functionally graded beams based on Timoshenko beam theory: Chebyshev collocation method', Meccanica, 50, pp. 1331–1342, 2015.

[27] F. Delale, F. Erdogan, 'The crack problem for a nonhomogeneous plane', ASME Journal of Applied Mechanics, 50, pp. 609–614, 1983.

[28] A.K. Niyogi, 'Nonlinear bending of rectangular orthotropic plates', International Journal of Solids and Structures, 9(9):1133–9, 1973.

[29] M. Bayat, I. Pakar, and G. Domairry, 'Recent developments of some asymptotic methods and their applications for nonlinear vibration equations in engineering problems: a review', Latin American Journal of Solids Structures, 9(2), pp. 145–234, 2012.
[30] J.H. He, 'Hamiltonian approach to nonlinear approach', Physics Letters A, 374, 2312–2314, 2010.

Biography

Dang Van Hieu received the bachelor's degree in Mechanical Engineering from VNU – University of Science in 2007, the master's degree in Solids Mechanics from VNU – University of Science in 2011, and the philosophy of doctorate degree in Solids Mechanics from VAST- Graduate University of Science and Technology in 2021, respectively. He is currently working as a Lecture at the Department of Mechanics, Faculty of Automotive and Power Machinery Engineering, TNU-Thai Nguyen University of Technology. His research areas include nonlinear vibration, random vibration and structural dynamics. He has been serving as a reviewer for many highly-respected journals.